Received: 29 October 2023 | *Revised:* 10 December 2023 | *Accepted:* 28 December 2023
DOI:10.37917/ijeee.20.1.20 *Vol. 20 | Issue 1 | June 2024*

Iraqi Journal for Electrical and Electronic Engineering
Original Article

Open Access
IJEEE University of Basrah College of Engineering

Improving Operating Time for External Laser Source based Polymer Fiber by Optimizing Model Parameters

Hisham Kadhum Hisham* and Ali Kamel Marzook
Electrical Engineering Department, University of Basrah, Basrah, Iraq

Correspondance
*Hisham Kadhum Hisham
Electrical Engineering Department
University of Basrah, Basrah, Iraq
Email: Husham_kadhum@yahoo.com

Abstract
In this paper, an analysis of performance acceleration of an external laser source (ELS) model based polymer fiber gratings (PFGs) by reducing the turn-on delay time (TDelay) is successfully investigated numerically by optimizing model parameters. In contrast to all previous studies that relied either on approximate or experimental equations, the analysis was based on an exact numerical formula. The analysis is based on the investigation of the effect of diode injected current (Iin j), temperature (T), recombination rate coefficients (i.e. Anr, B, and C), and optical feedback (OFB) level. Results have demonstrated that by optimizing model parameters the Delay can be controlled and reduced effectively.

Keywords
External Laser Source, Laser Delay Time, Numerical Analysis, Laser Dynamics, Polymer Grating Fiber (PGF).

I. Introduction

With the continuous revolutionary increase in the volume of transmitted data and the increasing demand for optical sensing technologies in many important applications, the need for a tunable laser with a wide range makes it possible for high potential and good efficiency to manage and transmit information [1][2], thus improving the ability of the network in front of the increasing traffic and at the same time its high ability to sense accurately is one of the most important goals that must be achieved as requirements for the next generation of optical transmission networks [3][4].

Recent years have witnessed a noticeable increase in the use of fiber gratings (FGs) in many fields due to their unique features, where external environmental conditions such as stress [5][6] and temperature [7][8][9] play a fundamental role in determining their basic parameters such as operating wavelength [10][11][12] and low dispersion loss [13][14][15]. Despite all these advantages, the limited tunability which is represent the main key for dense wavelength division multiplexing networks (DWDM) is a major drawback of silica fiber gratings (SFGs) [3][4][7].

However, the development in optical fiber manufacturing technology has made it possible to overcome this major point. Where, the optical fibers that made of a polymer materials have thermal and tensile properties that are much higher than that in the case of a SFGs [7]. The Young's modulus of the polymer is 70 times smaller than the Young's modulus of silica (i.e. $0.1 \times 10^{10} N/m^2$ compared to $7.13 \times 10^{10} N/m^2$) [7], which gives it a significant advantage in mechanical synthesis compared to that of a SFGs [7].

Also, the advantages of a wide thermo-optical effect give them a large ability to adjust the refractive index and thus a wide tuning range. Moreover, the high flexibility of polymer fiber gratings (PGFs) can make the tunability extend beyond the thermo-optical limit [3][4][7]. These unique features give the PGFs the highest advantage for use as a wavelength tuning and optical sensing element.

The huge increase in the use of DWDM networks has led to an increase in demand for using the external cavity lasers (ECLs) based FGs as an alternative light source for two important reasons: (1) their ability to generate a light with highly wavelength stability, where the emission wavelength of

the ECLs depends only on the Bragg wavelength of the FGs and does not depend on the injection current (I_{inj}) of the laser diode cavity [16][17][18][19][20] and (2) the high ability to control the operating wavelength for the FGs more precisely and with great flexibility compared with other laser models [21].

One of the most important parameters that determines the dynamic performance for the semiconductor laser diodes (SLDs) is the turn-on delay time (T_Delay) [22][23][24][25][26] [27]. It defined as the time required for carriers (N) to populate and to reach its threshold level (N_{th}) at which the initial value of current (I_o) changes to any current (I) greater than its threshold level (I_{th}) [22][23]. In this period, photon concentrations (P) suffer from a relaxation fluctuation until they reach their steady-state value [24][25].

Experimentally, the value of T_{Delay} is strongly determined by the value of the carrier recombination rate coefficients (i.e. A_{nr}, B and C) [26][27]. However, previous studies have relied in their analysis either on an approximated or an empirical relationship [24] or on equations in which one or more parameters that have an important influence on their behavior have been neglected [25]. In [28], the authors modeled the turn-on delay as an parabolic arc approximation and in [29], the authors have studied the turn-on time delay under the limiting case where the A_{nr} recombination dominates. While in [30], The authors showed that the effect of the A_{nr}, B and C parameters was to reduce the delay time, which was later shown to be inaccurate [31]. These hypotheses, in addition to the inaccuracy of the results, have eliminated the effect of some important parameters that have an impact in determining the true dynamic behavior of the system [26][27]. Moreover, to the best of our knowledge, all the previous studies that addressed this important parameter have concerned on the fiber lasers based SFGs [24][25][26][27].

The growing fields of optical sensing compared to other sensing technologies [21] and the diversity of promising applications within optical communication systems make from the PFGs an important tool sensing applications [32][33][34][35] [36] [37]. So, studying the dynamic properties of ELS based PFGs is necessary and of great interest.

II. Turn-on delay time of ELS based PFGs

A schematic diagram of a ELS model based PFGs is shown in Fig. 1. The model is consisting of a 1.55 μm Fabry-Perot (FP) laser diode coupled to a single-mode fiber with L_{ext} length with C_o coupling coefficient and a PFGs of length L_{FG} and R_{FBG} reflectivity.

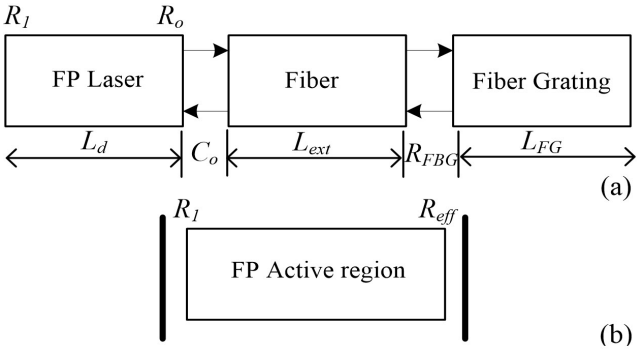

Fig. 1. (a) structure of external laser source based Plastic fiber gratings model and (b) Simplified configuration [16][38]

According to Fig. 1, the effective reflectivity (R_{eff}) of PFGs is given by [38]

$$R_{eff} = \frac{R_o^2 + R_{OFB}^2 + 2R_o R_{OFB}\cos(\omega\tau_e)}{1 + R_o^2 R_{OFB}^2 + 2R_o R_{OFB}\cos(\omega\tau_e)} \tag{1}$$

In Eq. 1, $\omega\tau_e$ represent the phase of the light that reflected, $R_{OFB} = C_o R_{ext}$ represent the optical

$$R_{\text{ext}} = |R_{FBG}|^2 = \begin{cases} \frac{(kL_{FG})^2 \sinh^2(QL_{FG})}{(\Delta\beta L_{FG})^2 \sinh^2(QL_{FG}) + (QL_{FG})^2 \cosh^2(QL_{FG})}, \\ \text{if} \quad (kL_{FG})^2 \rangle (\Delta\beta L_{FG})^2 \\ \frac{(kL_{FG})^2 \sin^2(\Omega L_{FG})}{(\Delta\beta L_{FG})^2 - (kL_{FG})^2 \cos^2(\Omega L_{Fg})}, \\ \text{if} \quad (kL_{FG})^2 \langle (\Delta\beta L_{FG})^2 \end{cases} \tag{2}$$

In Eq.2, $\Delta\beta$ represent the wavelength detuning, k is the coupling strength, $Q = \sqrt{k^2 - \Delta\beta^2}$, and $\Omega = iQ = \sqrt{\Delta\beta^2 - k^2}$ [7][38]. By taking into account the phase change in Eq. 1, R_{eff} can be rewritten as

$$R_{eff} = \frac{R_o^2 + R_{OFB}^2 + 2R_o R_{OFB}\cos(\omega\tau_e - \Theta_{ref})}{1 + R_o^2 R_{OFB}^2 + 2R_o R_{OFB}\cos(\omega\tau_e - \Theta_{ref})} \tag{3}$$

Where Θ_{ref} represent the phase coefficient for light reflected and is given by[16][21][38]

$$\Theta_{ref} = \begin{cases} \tan^{-1}\left(\frac{Q\cosh(QL_{FG})}{\Delta\beta\sinh(QL_{FG})}\right) & ,if(kL_{FG})^2 > (\Delta\beta L_{FG})^2 \\ \tan^{-1}\left(\frac{\Omega\cos(\Omega L_{FG})}{\Delta\beta\sin(\Omega L_{FG})}\right) & ,if(kL_{FG})^2 < (\Delta\beta L_{FG})^2 \end{cases} \tag{4}$$

The threshold current $I_{th,fe}(T)$ of ELS based FPGs after considering the temperature dependence (TD) and OFB can be written as [24][25][38]

$$I_{th,fe}(T) = qVN_{th,fe}(T)\left(A_{nr} + BN_{th,fe}(T) + C(T)N^2_{th,fe}(T)\right) \quad (5)$$

In Eq. 5,$q,V,A_{nr},C(T),B$ and $N_{th,fe}(T)$ are represents the charge of electron, volume of FP active region, non-feedback (OFB) reflected light that coupled into FP laser, and R_{ext} is the power reflectivity of grating fiber which is defined as [16][21][38] radiative recombination rate, Auger process, radiative recombination coefficient, and carrier density at the threshold condition which is defined by [38]

$$N_{th,fe}(T) = N(T) + \frac{1}{\Gamma v_g(T)a(T)\tau_{p,fe}(T)} \quad (6)$$

where $N(T)$ is the transparency carrier density, a(T) is the gain coefficient, and $\tau_{p,fe}(T)$ is the photon life time,Γ is the confinement factor, and $v_g(T) = c/n_d(T)$ is the group velocity, respectively [16][21][38]. In Eq. 6, $\tau_{p,fe}(T)$ can be modeled as [38]

$$\tau_{p,fe}(T) = \frac{1}{v_g(T)\alpha_{tot,fe}(T)} \quad (7)$$

In Eq. 7, $\alpha_{tot,fe}(T)$ is the total FP cavity loss which is defined by [16][24][25][38].

$$\alpha_{tot,fe}(T) = \alpha_{int}(T) + \frac{1}{2L_d}\ln(\frac{1}{R_1R_{eff}}) \quad (8)$$

where $\alpha_{int}(T)$ represent the internal FP cavity loss, and $\frac{1}{2L_d}\ln(\frac{1}{R_1R_{eff}})$ is the FP mirror loss [24][25]. Finally, the $N_{th,fe}$ can be expressed as

$$\begin{aligned} &N_{th,fe}(T) \\ &= N(T) + \frac{1}{\Gamma a(T)}\left[\alpha_{int}(T) + \frac{1}{2L_d}\left\{\ln(\frac{1}{R_1})\right.\right. \\ &\quad \left.\left. + \ln(\frac{1 + 2R_oR_{OFB}\cos(\omega\tau_e - \Theta_{ref}) + R_o^2R_{OFB}^2}{R_o^2 + 2R_oR_{OFB}\cos(\omega\tau_e - \Theta_{ref}) + R_{OFB}^2})\right\}\right] \end{aligned} \quad (9)$$

The well-known formula that described the T_{Delay} response of a SLD is defined by [25]

$$T_{Delay} = \int_{N_i}^{N_{th}} \frac{qV}{I_{inj} - qVN(A_{nr} + BN + CN^2)}dN \quad (10)$$

Eq. 10 have been solved numerically (See Appendix A) after considering the effect of the R_{eff} which is defined in Eq. 1 to study the T_{Delay} characteristics of ELS model based PFGs.

TABLE I.
Parameters of ELS based PFGs at room temperature [21] [24] [25] [26][31][37][38]

Parameter	Description
$L_d = 400\mu m$	Cavity length
$d = 0.1\mu m$	Active region thickness
$w = 2\mu m$	Active region width
$N_o = 1.10^{24}m^{-3}$	Transparency carrier density
$A_{nr} = 1.10^8 sec^{-1}$	Non-radiative recombination coefficient
$B = 1.10^{-16}m^3/sec$	Radiative recombination coefficient
$C = 3.10^{-41}m^6/sec$	Auger recombination coefficient
$\alpha_{int} = 1000m^{-1}$	Internal cavity loss
$R_1 = 0.99$	Reflectivity of the left facet
$a = 2.5 \times 10^{-20}m^2$	Gain constant
$L_{FG} = 4mm$	Grating length

III. Results and discussion

Table I show the common values for ELS based PFGs model are used in the analysis.

Figure 2 show the T_{Delay} response for an ELS based PFGs model as a function to the ρ parameter for different values of σ parameter. Results shown that, by increasing the ρ value, the value of T_{Delay} has reduced. These results are fully consistent with the basic principles of laser operation, which are when the laser has biased near the N_{th} value, the T_{Delay} response can be eliminated [24][25].

To illustrate the differences in accuracy in the method we adopted in our analysis (i.e. Eq. A.1) compared to other approximated relationships, equations and expressions in the previous study [24][25][26][27][28][29][30], Fig. 3 shows the effect of the parameters have been neglected on the T_{Delay} responses. The difference in the results is clear and this is expected, and it is surprising how the influence of an important parameters have been ignored in the previous studied [24][25][26][27][28][29][30], where according to Eq. 5, any increase in A_{nr}, B, and C parameters will lead to an increase in the I_{th} value (i.e. Eq. 5)). As it is known [24, 25], the higher the I_{th} value, the greater T_{Delay} level. This meaning that, the effect of increasing any one of the Anr, B, and C coefficients is to increase the T_{Delay} response value as shown in Fig. 4.

One of the most important parameters that affect the dynamic behavior of lasers is the change in temperature [24][25]. The effect of temperature (T) variation on the T_{Delay} response for the ELS based PFGs is shown in fig. 5. By increasing the T value, the T_{Delay} response is increases. The reason for this is due to its direct impact on the N_{th} value as given in Eq. 6. However, this effect can be eliminated by increasing the ρ value. Where by increasing the ρ value (i.e. $\rho \to 1$) the value of N_i will reach to N_{th} and this leads to mitigate T_{Delay} (i.e.$T_{Delay} \to 0$). Thus, the ρ value is represented a

significant/or control parameter for reducing the T_{Delay}.

On the other hand, by increasing of the σ value, the T_{Delay} value is reduced at a specified value of the ρ parameter; thus, the effect of temperature can be controlled.

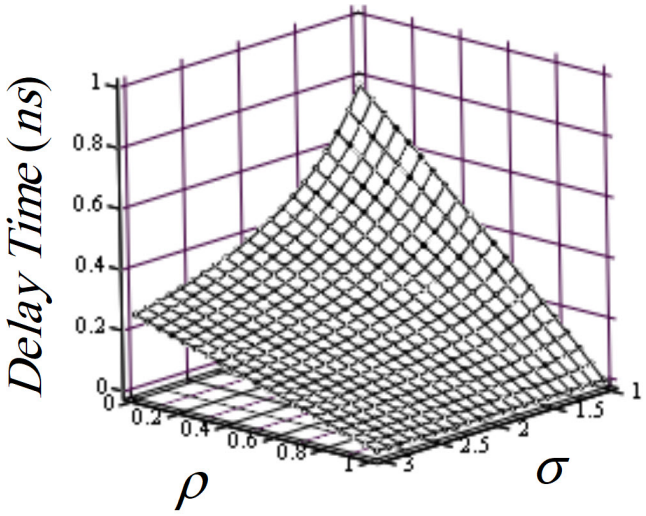

Fig. 2. Effect of ρ and σ parameters on T_{Delay} response.

Figure 6 show the effect of the external optical feedback (EOF) reflectivity; R_{ext} on the T_{Delay} response as a function of σ at $\rho = 0.5$. . As is clear, the effect of increasing reflectivity works effectively in reducing the T_{Delay} value. This is due to their effect on decreasing the total cavity losses (Eq. 8), which in turn leads to an increase in the photons lifetime Eq. 7, which is leads in decreasing in the value of threshold current Eq.5 and thus reducing the delay time. Depending on this result, the value of EOF can be used as a controller to turn-on the laser by controlling the N_{th} level.

IV. Conclusions

In this paper, an analysis on improving the operating time of an external laser source (ELS) based polymer fiber gratings (PFGs) model depending on reducing the turn-on time delay (T_{Delay}) has been investigated numerically. In our analysis, in contrast to the methods that were adopted in all previous studies, we did not use an approximate or empirical equations, but rather relied on an accurate numerical formula. Results show that the A_{nr}, B and C coefficients have a significant effect on the T_{Delay} value and not as reported in the previous study [30]. Also, result show that, the effect of temperature is to increase the T_{Delay} value. However, this effect can be eliminated either by increasing ρ value or by increasing σ value at a constant I_{th}. On the other hand, the T_{Delay} value can be controlled through controlling the external optical feedback (EOF) level.

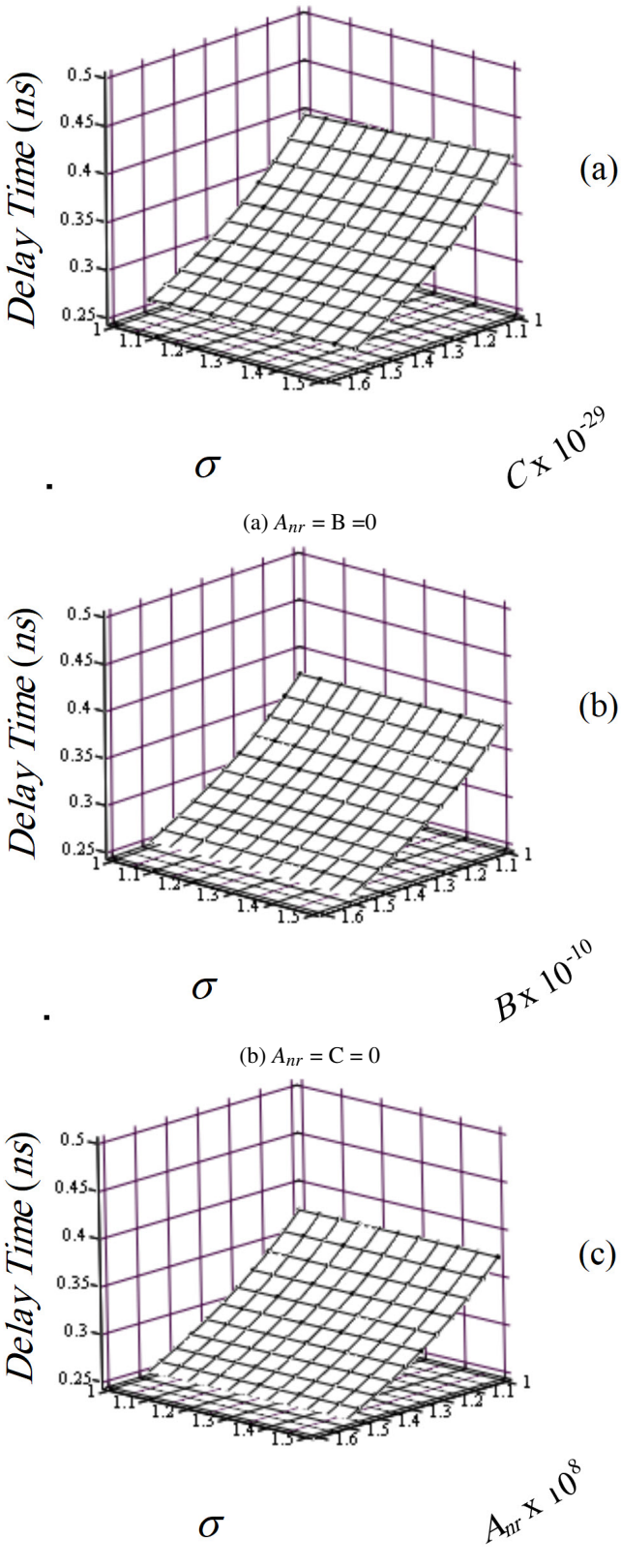

(a) A_{nr} = B =0

(b) A_{nr} = C = 0

(c) B = C = 0

Fig. 3. Effect of neglected A_{nr}, B, and C parameters on T_{Delay} value with σ at $\rho = 0.5$

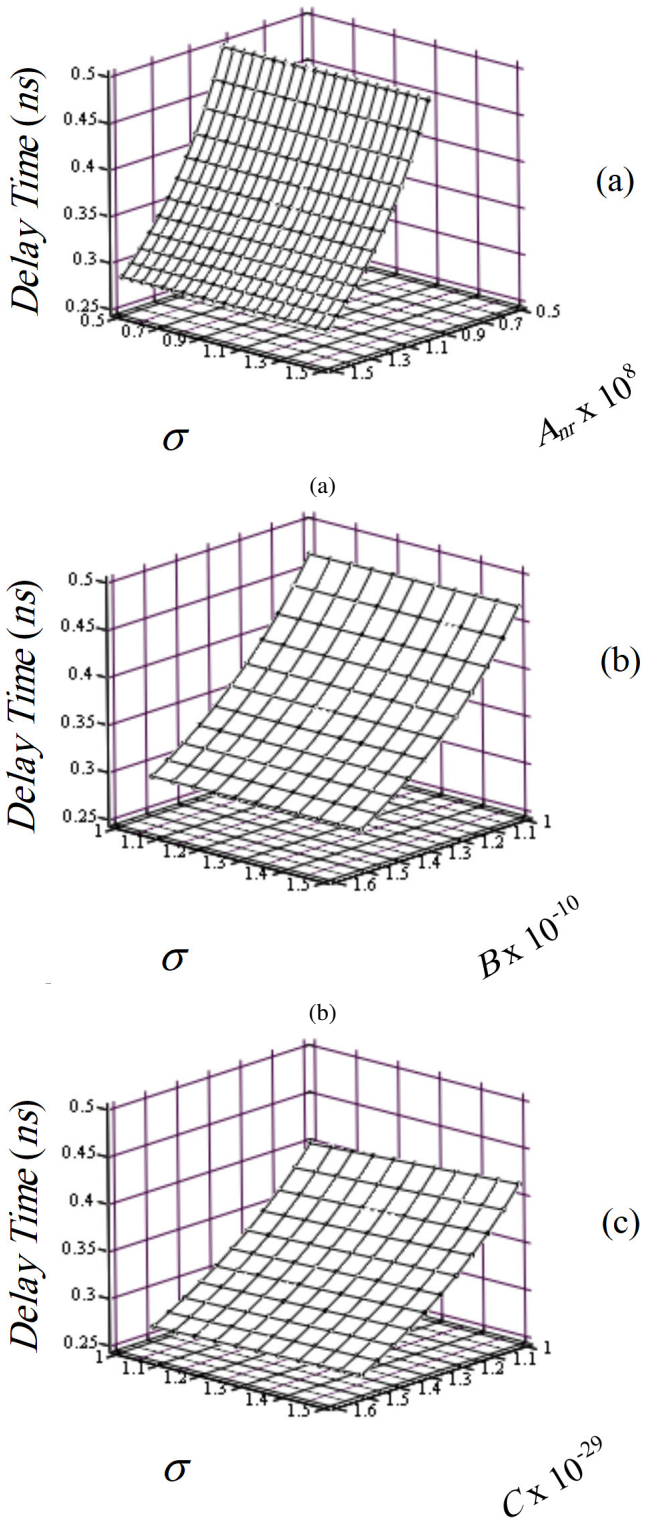

Fig. 4. Effect of A_{nr}, B, C coefficients and σ on turn-on time delay at $\rho = 0.5$.

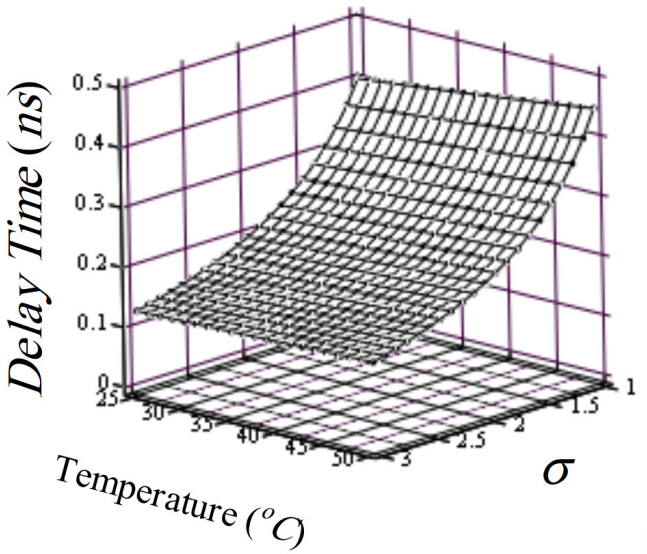

Fig. 5. Effect of temperature on T_{Delay} and σ at $\rho = 0.5$.

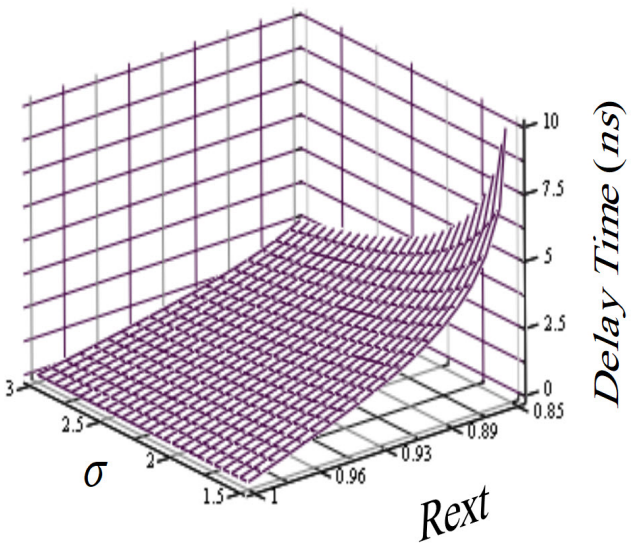

Fig. 6. . Effect of R_{ext} and σ parameter on turn-on time delay at $\rho = 0.5$.

APPENDIX A

The numerical solution of Eq. 10 is given by [23, 27]

$$T_{\text{Delay}} = \psi\Re_1 \text{ T1} + \psi\Re_2 \text{ T2} + \psi\Re_3 \text{ T3} \tag{A.1}$$

Where

$$\text{T1} = \ln\left[\frac{\hbar\left(\Re_1, N_{th,\text{ OFB}}\right)}{\hbar\left(\Re_1, \rho N_{th,\text{ OFB}}\right)}\right] \tag{A.2}$$

$$\mathrm{T2} = \ln\left[\frac{\hbar\left(\Re_2, N_{th,\mathrm{OFB}}\right)}{\hbar\left(\Re_2, \rho N_{th,\ \mathrm{OFB}}\right)}\right] \tag{A.3}$$

$$\mathrm{T3} = \ln\left[\frac{\hbar\left(\Re_3, N_{th,\mathrm{OFB}}\right)}{\hbar\left(\Re_3, \rho N_{th,\mathrm{OFB}}\right)}\right] \tag{A.4}$$

$$\hbar\left(\Re_m, N\right) = B + \lambda 1 \Re_m + \lambda 2 N \tag{A.5}$$

$$\lambda 1 = \left(A_n B \xi + 9 C I_{inj}\right) \tag{A.6}$$

$$\lambda 2 = \left[\left(2B^2 - 6A_{nr}C\right) \Leftarrow \Re_m + 3C\right] \tag{A.7}$$

$$\Re_1 = \frac{1}{6\xi}\frac{\wp_2}{\wp_1} + 2\left(3A_{nr}C - B^2\right)\frac{\xi}{\wp_4} \tag{A.8}$$

$$\Re_2 = \frac{-1}{2}\aleph 1 + j\frac{\sqrt{3}}{2}\aleph 1 \tag{A.9}$$

$$\Re_3 = \frac{-1}{2}\aleph 1 - j\frac{\sqrt{3}}{2}\aleph 1 \tag{A.10}$$

$$\aleph 1 = \left(\frac{1}{6\xi}\frac{\wp_2}{\wp_1} + 2\left(3A_{nr}C - B^2\right)\frac{\xi}{\wp_4}\right) \tag{A.11}$$

$$\wp_1 = \xi^2 A_{nr}^2 \Theta 1 + \xi I_{inj} \Theta 2 + 27 C^2 I_{inj}^2 \tag{A.12}$$

$$\Theta 1 = \left(4A_{nr}C - B^2\right) \tag{A.13}$$

$$\Theta 2 = \left(18A_{nr}C - 4B^2\right) \text{ (A. 13)} \tag{A.14}$$

$$\wp_2 = \left[\xi^2 \wp_1 \left(-108C + 12\sqrt{3}\wp_3^{1/2}\right)\right]^{1/3} \tag{A.15}$$

$$\wp_3 = \frac{\wp_4}{\wp_1} \tag{A.16}$$

$$\wp_4 = 4\xi^2 B^2 \Theta 3 + 108\xi^2 C^2 I_{inj} \Theta 4 + 729 C^4 I_{inj}^2 \tag{A.17}$$

$$\Theta 3 = \left(20.25A_{nr}^2 C^2 - 9A_{nr}B^2 C + B^4\right) \tag{A.18}$$

$$\Theta 4 = \left(4.5A_m C - B^2\right) \tag{A.19}$$

And $\xi = eV$ and $\rho(0 < \rho(1)$ represents the ratio of the N_i to the N_{th} value (i.e. $\rho = N_i/N_{th}$).

CONFLICT OF INTEREST

The authors have no conflict of relevant interest to this article.

REFERENCES

[1] Y. Fan, J. Liu, R. Xiao, Y. Gong, Z. Sun, P. Dai, K. Tang, Y. Shi, and X. Chen, "Uncooled tunable laser based on high-density integration of distributed feedback semiconductor lasers," *IEEE Journal of Quantum Electronics*, 2023.

[2] Z. Sun, Z. Su, R. Xiao, Y. Wang, K. Liu, F. Wang, Y. Liu, T. Fang, Y.-J. Chiu, and X. Chen, "Tunable laser via high-density integration of dfb lasers with high precision wavelength spacings," *IEEE Photonics Technology Letters*, vol. 34, no. 9, pp. 467–470, 2022.

[3] M. Khan, "Quantum-dash laser-based tunable 50/75 ghz mmw transport system for future l-band networks," *IEEE Photonics Technology Letters*, vol. 34, no. 16, pp. 842–845, 2022.

[4] Z. Wei, J. Zhang, W. Li, and D. V. Plant, "400-gbps/80-km rate-flexible pcs-64-qam wdm-cpon with pseudo-m-qam chaotic physical layer encryption," *Journal of Lightwave Technology*, vol. 41, no. 8, pp. 2413–2424, 2023.

[5] T. Tan, Y. Xie, C. Duan, Q. Chai, Y. Chu, G. Sun, Y. Luo, Y. Tian, and J. Zhang, "Accuracy improvement of residual stress measurements in the tube by fbg using the genetic algorithm," *IEEE Transactions on Instrumentation and Measurement*, vol. 71, pp. 1–7, 2022.

[6] J. Zhang, T. Tan, C. Duan, Z. Li, X. Liu, Q. Chai, G. Xiao, Y. Tian, W. Zhang, and Y. Xu, "Measurement of residual stress based on a ring fbg array," *IEEE Transactions on Instrumentation and Measurement*, vol. 71, pp. 1–7, 2021.

[7] H. K. Hisham, "Numerical analysis of thermal dependence of the spectral response of polymer optical fiber bragg gratings.," *Iraqi Journal for Electrical & Electronic Engineering*, vol. 12, no. 1, 2016.

[8] Y.-L. Wang, Y. Tu, and S.-T. Tu, "Development of highly-sensitive and reliable fiber bragg grating temperature sensors with gradient metallic coatings for cryogenic temperature applications," *IEEE sensors journal*, vol. 21, no. 4, pp. 4652–4663, 2020.

[9] Y. Zhao, S. Liu, J. Luo, Y. Chen, C. Fu, C. Xiong, Y. Wang, S. Jing, Z. Bai, C. Liao, *et al.*, "Torsion, refractive index, and temperature sensors based on an improved helical long period fiber grating," *Journal of Lightwave Technology*, vol. 38, no. 8, pp. 2504–2510, 2020.

[10] S. Chen, Y. Zhao, M. Tang, Z. Hua, H. Peng, Y. Ma, and Y. Liu, "Wavelength selective mode conversion in few-mode fiber with cascaded long-period gratings," in *2022 Asia Communications and Photonics Conference (ACP)*, pp. 218–221, IEEE, 2022.

[11] Z. Liu, X. Zhao, C. Mou, and Y. Liu, "Mode selective conversion enabled by the long-period gratings inscribed in elliptical core few-mode fiber," *Journal of Lightwave Technology*, vol. 38, no. 6, pp. 1536–1542, 2020.

[12] N. Deng, L. Zong, H. Jiang, Y. Duan, and K. Zhang, "Challenges and enabling technologies for multi-band wdm optical networks," *Journal of Lightwave Technology*, vol. 40, no. 11, pp. 3385–3394, 2022.

[13] H. Wang, Y. Liang, X. Zhang, S. Chen, L. Shen, L. Zhang, J. Luo, and J. Wang, "Low-loss orbital angular momentum ring-core fiber: design, fabrication and characterization," *Journal of lightwave technology*, vol. 38, no. 22, pp. 6327–6333, 2020.

[14] P. Zhu, P. Liu, Z. Wang, C. Peng, N. Zhang, and M. A. Soto, "Evaluating and minimizing induced microbending losses in optical fiber sensors embedded into glass-fiber composites," *Journal of lightwave technology*, vol. 39, no. 22, pp. 7315–7325, 2021.

[15] C. Xia, Z. Deng, A. Zhang, P. Cai, Z. Mo, J. Liu, G. Zhou, Z. Hou, Q. Zhang, and L. Guo, "Ultra-low-loss hollow-core bragg antiresonant fiber with super bandwidth transmission window," *IEEE Photonics Journal*, vol. 14, no. 3, pp. 1–5, 2022.

[16] H. K. Hisham, A. F. Abas, G. A. Mahdiraji, M. A. Mahdi, and A. S. M. Noor, "Relative intensity noise reduction by optimizing fiber grating fabry–perot laser parameters," *IEEE Journal of Quantum Electronics*, vol. 48, no. 3, pp. 375–383, 2011.

[17] D. Priante, M. Zhang, A. R. Albrecht, R. Bek, M. Zimmer, C. L. Nguyen, D. P. Follman, G. D. Cole, and M. Sheik-Bahae, "In-well pumping of a membrane external-cavity surface-emitting laser," *IEEE Journal of Selected Topics in Quantum Electronics*, vol. 28, no. 1: Semiconductor Lasers, pp. 1–7, 2021.

[18] Y. Wu, L. Deng, K. Yang, and W. Liang, "Narrow linewidth external cavity laser capable of high repetition frequency tuning for fmcw lidar," *IEEE Photonics Technology Letters*, vol. 34, no. 21, pp. 1123–1126, 2022.

[19] X. Qiu, C. Wang, J. Li, C. Li, X. Xie, Y. Wang, and X. Wei, "Temperature-stabilized and widely tunable vertical external cavity surface-emitting laser with a simple line cavity," *IEEE Photonics Journal*, vol. 14, no. 4, pp. 1–7, 2022.

[20] P. Tatar-Mathes, H.-M. Phung, A. Rogers, P. Rajala, S. Ranta, M. Guina, and H. Kahle, "Effect of non-resonant gain structure design in membrane external-cavity surface-emitting lasers," *IEEE Photonics Technology Letters*, 2023.

[21] H. Hisham, *Fiber bragg grating sensors: development and applications*. CRC Press, 2019.

[22] H. K. Hisham, S. B. A. Anas, M. H. A. Bakar, M. T. Alresheedi, A. F. Abas, and M. A. Mahdi, "Parametric study of the transient period characteristics of distributed feedback laser diodes," *Journal of Optical Technology*, vol. 90, no. 2, pp. 68–74, 2023.

[23] H. K. Hisham, "Delay time reduction in vcsels by optimizing laser parameters.," *Iraqi Journal for Electrical & Electronic Engineering*, vol. 12, no. 2, 2016.

[24] M. M.-K. Liu, "Principles and applications of optical communications," *(No Title)*, 1996.

[25] G. P. Agrawal and N. K. Dutta, "Semiconductor lasers, 2nd ed. new york, ny, usa: van nostrand reinhold," 1993.

[26] H. Hisham, G. Mahdiraji, A. Abas, M. Mahdi, and F. M. Adikan, "Characterization of transient response in fiber grating fabry–perot lasers," *IEEE Photonics Journal*, vol. 4, no. 6, pp. 2353–2371, 2012.

[27] H. K. Hisham, G. A. Mahdiraji, A. Abas, M. A. Mahdi, and F. M. Adikan, "Characterization of turn-on time delay in a fiber grating fabry–perot lasers," *IEEE Photonics Journal*, vol. 4, no. 5, pp. 1662–1678, 2012.

[28] S. Betti, E. Bravi, and M. Giaconi, "Effect of the turn-on delay of a semiconductor laser on clipping impulsive noise," *IEEE Photonics Technology Letters*, vol. 9, no. 1, pp. 103–105, 1997.

[29] N. Volet and E. Kapon, "Turn-on delay and auger recombination in long-wavelength vertical-cavity surface-emitting lasers," *Applied Physics Letters*, vol. 97, no. 13, 2010.

[30] X. Zhang, W. Pan, J. Chen, and H. Zhang, "Theoretical calculation of turn-on delay time of vcsel and effect of carriers recombination," *Optics & Laser Technology*, vol. 39, no. 5, pp. 997–1001, 2007.

[31] H. Hisham, A. Abas, G. A. Mahdiraji, M. Mahdi, and A. M. Noor, "Comment on:"theoretical calculation of turn-on delay time of vcsel and effect of carriers recombination"[opt. laser technol. 39 (2007) 997–1001]," *Optics & Laser Technology*, vol. 44, no. 6, pp. 1995–1998, 2012.

[32] L. Pereira, C. Marques, R. Min, G. Woyessa, O. Bang, H. Varum, and P. Antunes, "Bragg gratings in zeonex microstructured polymer optical fiber with 266 nm nd: Yag laser," *IEEE Sensors Journal*, 2023.

[33] R. He, C. Teng, S. Kumar, C. Marques, and R. Min, "Polymer optical fiber liquid level sensor: A review," *IEEE Sensors Journal*, vol. 22, no. 2, pp. 1081–1091, 2021.

[34] T. Cheng, B. Li, F. Zhang, J. Chen, Q. Zhang, X. Yan, X. Zhang, T. Suzuki, Y. Ohishi, and F. Wang, "A surface plasmon resonance optical fiber sensor for simultaneous measurement of relative humidity and temperature," *IEEE Sensors Journal*, vol. 22, no. 4, pp. 3246–3253, 2022.

[35] H. Yin, Z. Shao, F. Chen, and X. Qiao, "Highly sensitive ultrasonic sensor based on polymer bragg grating and its application for 3d imaging of seismic physical model," *Journal of Lightwave Technology*, vol. 40, no. 15, pp. 5294–5299, 2022.

[36] H. K. Hisham, G. A. Mahdiraji, A. Abas, M. A. Mahdi, and F. M. Adikan, "Characterization of turn-on time delay in a fiber grating fabry–perot lasers," *IEEE Photonics Journal*, vol. 4, no. 5, pp. 1662–1678, 2012.

[37] H. K. Hisham, "Numerical analysis of thermal dependence of the spectral response of polymer optical fiber bragg gratings.," *Iraqi Journal for Electrical & Electronic Engineering*, vol. 12, no. 1, 2016.

[38] H. Hisham, A. Abas, G. A. Mahdiraji, M. Mahdi, and A. M. Noor, "Improving the characteristics of the modulation response for fiber bragg grating fabry–perot lasers by optimizing model parameters," *Optics & Laser Technology*, vol. 44, no. 6, pp. 1698–1705, 2012.